Welding in the World
https://doi.org/10.1007/s40194-025-02191-3

RESEARCH PAPER

Statistical correlation of 3D scanned weld geometry distributions and fatigue life for different welding methods

Martin Leonel Melucci[1] · Sulaiman Shojai[1] · Mahamudul Hasan Tanvir[1] · Moritz Braun[1,2]

Received: 21 July 2025 / Accepted: 29 September 2025

Abstract
The relationship between local weld geometry and fatigue life has been extensively studied over the past decades, driven by the need to enhance structural integrity and optimize costs throughout a structure's service life. While numerous studies have explored the influence of weld geometry on fatigue strength, the comparative effect of different welding methods under comparable weld geometry quality remains largely unexplored. Furthermore, the influence of local geometric variations for each welding method has not been systematically evaluated. This study explores a large dataset of laser-scanned butt welds, analyzing key geometric parameters. The dataset is categorized by welding method (laser-hybrid welding, submerged arc welding, and flux core arc welding), and statistical distributions are examined to assess variations in weld geometry and compliance with ISO 5817 quality groups. The characteristic fatigue life for each quality group is estimated. The correlation between geometric factor and fatigue life is evaluated through the residual analysis of stress-life curve linear fitting. According to the findings, different geometry features dominate depending on the welding method. The fracture location is strongly influenced by angular misalignment, while fatigue strength is better explained by quantile-based analysis of local geometry. These results provide a basis for future predictive modeling and quality assessment in welded structures.

Keywords Butt-weld · 3D scans · Weld quality · Statistical assessment · Fatigue strength

Nomenclature

t, t_L, and t_R	Thickness, left and right thickness
e	Axial misalignment
φ	Angular misalignment
TL, TR	Top left notch, top right notch
BL, BR	Bottom left notch, bottom right notch
W_T and W_B	Weld width top and bottom side
H_T and H_B	Weld height top and bottom side
r_{TL}, r_{TR}, r_{BL}, and r_{BR}	Weld toe radius: top left, top right, bottom left, bottom right
α_{TL}, α_{TR}, α_{BL}, and α_{BR}	Notch angle: top left, top right, bottom left, bottom right
d_{TL}, d_{TR}, d_{BL}, and d_{BR}	Undercut depth: top left, top right, bottom left, bottom right

Recommended for publication by Commission XV - Design, Analysis, and Fabrication of Welded Structures

✉ Martin Leonel Melucci
martin.melucci@dlr.de

Sulaiman Shojai
sulaiman.shojai@dlr.de

Mahamudul Hasan Tanvir
mahamadul.tanvir@dlr.de

Moritz Braun
moritz.braun@dlr.de

[1] German Aerospace Center (DLR), Institute of Maritime Energy Systems, Geesthacht, Germany

[2] Institute for Ship Structural Design and Analysis, Hamburg University of Technology, Hamburg, Germany

1 Introduction

Over the past few decades, significant attention has been directed toward understanding the impact of weld geometry on fatigue life. This interest originates from the importance of improving structural reliability while optimizing manufacturing together with maintenance costs and recently to meet sustainability objectives. Welded joints are employed in many industries, including automotive, aerospace [1], wind energy [2], ship building [3] and civil engineering [4, 5], where fatigue failure is one of the primary threats due to the cyclic loading conditions during service. The stress concentration due to the weld seam geometric discontinuities is a critical aspect, as these concentrations lead to crack initiation and can determine the fatigue life of a welded structure. As a result, research has increasingly focused on how specific geometric features influence fatigue performance and how these insights can guide both design and quality control.

For butt-welded joints, the local weld geometry is often characterized by parameters such as undercut depth, toe radius, flank angle, overfill height, and axial as well as angular misalignments [6–8]. These parameters have been identified as significant factors influencing the fatigue performance of welded specimens in numerous studies and are used as quality criteria in international standards such as ISO 5817 [9]. These criteria were set from a production point of view and showed in many studies a weak relation with actual fatigue life [10]. Therefore, new quality systems have been developed in the last years; for instance, the Volvo Group quality standard based on the works of Barsoum et al. [1] and the Annex B from the review of ISO 5817 [9] based on the works from Hobbacher and Kassner [11]. In Annex B, new assessment criteria were included to relate the quality groups B and C with fatigue design (FAT) classes.

Advancements in digital weld quality measurement techniques, such as 3D laser scanning, have allowed more precise and efficient characterization of the external weld geometries. These tools enable the development of predictive models that incorporate geometric features into fatigue strength assessment [12]. Finite element methods (FEM) have been widely applied to simulate stress distributions from scanned weld geometries and search for relations with the fatigue life of specimens [10, 13, 14].

Different studies have focused on finding correlations from scanned welds through stress concentration estimations or data-driven methods using machine learning. The influence of local weld geometry on fatigue crack initiation and fatigue strength in laser-hybrid joints was studied by Niraula et al. [15]. Their findings identified undercut depth as the most critical factor, with fatigue cracks consistently initiating at the location of the deepest undercut. In terms of fatigue performance, the undercut average depth was found to be suitable for fatigue strength characterization.

Likewise, Schork et al. [6, 14, 16] analyzed weld seams produced using tungsten inert gas welding (TIG) and gas metal arc welding (MAG) techniques; they identified the undercut depth as the most influential factor affecting the FAT class of butt welds, followed by flank angle and toe radius. The overfill height was found to have a smaller effect, and combined geometric factors influenced fatigue life more than individual ones. Moreover, low flank angle showed a beneficial effect on fatigue life. However, the statistical variation in geometry parameters was not considered in this analysis.

Schubnell et al. evaluated the fatigue life of 3D-scanned welded specimens using the IBESS fracture mechanic-based fatigue life prediction approach presented by Schork et al. [12]. The specimens analyzed were obtained by submerged arc welding (SAW), flux-cored arc welding (FCAW), laser and laser-hybrid (LH), and gas metal arc welding (GMAW) processes. They found a clear correlation between flank angle and fatigue strength for butt welds; however, on the contrary, no strong correlation was found with toe radius or undercut depth. They observed that these results may be influenced by the use of theoretical normal distributions, which do not accurately represent the actual skewed distributions according to Braun et al.'s observations [17].

Recently, Glienke et al. [10] found that axial misalignment and plate thickness significantly influence the fatigue strength of scanned SAW small welded butt joints and wind turbine components. Their study showed that SAW joints can achieve a FAT-class 100 (with slope $m = 3$) if ISO 5817 quality level B is met. They identified interactions between axial misalignment and thickness on their effect on fatigue life. However, weld overfill and toe angle were found to impact fatigue strength independently of plate thickness. Additionally, Renken et al. [7] have studied the quality class and stress concentration factor in dependence on the sampling rate in scanned fillet welds. They observed that using the modal value of the geometric factors in stress concentration calculations is not conservative and showed a need to agree on a quantile of the critical value to be used in these estimations.

Braun et al. used machine learning algorithms to assess interactions of geometric parameters and estimate stress concentration factors as well as failure locations and fatigue life. They applied gradient boosted trees to predict failure locations and fatigue life from laser scanned GMAW, FCAW, and SAW butt welds. Through explainable machine learning, they found that the height in the top side and the undercut depth were the most influential weld geometry factors to the fatigue life [18]—only exceeded by stress amplitude, maximum stress, and misalignment.

Despite significant progress, there are contradictory findings in the literature about the influence of the individual geometry parameters in the fatigue life of butt-welded specimens. In addition to local weld geometry, the fatigue performance of welded joints is influenced by numerous interacting factors. These include the applied load levels, residual stresses, microstructural properties, material strength, and environmental conditions [19, 20].

Although the influence of weld geometry on fatigue strength has been widely studied, the effect of different welding methods under comparable weld geometry quality remains largely unexplored. Moreover, how each welding method responds to local geometric variations has yet to be systematically assessed. The objective of this study is to identify the most appropriate statistical parameter for fatigue life estimation and evaluate its applicability across a range of welded specimens. To address the identified research gap, this work systematically analyzes the influence of local geometric variations on fatigue performance for SAW, FCAW, and LH welded specimens (their typical cross sections are presented in Fig. 1). The evaluation was carried out within a consistent statistical framework that integrated regression diagnostics and hypothesis testing. This approach ensured robustness by considering a wide range of statistical metrics, rather than relying on isolated observations.

The correlation between geometric parameters and fatigue life is examined through residual analysis of linear stress-life (S–N) curve fitting specific to each welding method. While this type of residual analysis has been applied to evaluate the effects of temperature [21] and loading conditions [22] on fatigue life, the novelty of the present study lies in its application to assess the impact of local weld geometry. This study does not explicitly account for geometry-driven stress concentrators. Its primary aim is to identify statistically representative parameters for fatigue life estimation, which can subsequently be used to calculate stress concentration factors and weld quality assessment.

2 Dataset

Different welding methods, thicknesses, and steel types were selected to rule out uncertainties related to the former and to create a large database for the assessment of the correlations between local weld geometry and fatigue of butt-welded joints. The specimens analyzed were saw-cut from butt-welded plates into 40-mm-wide and 500-mm-long strips from previous and ongoing research projects from Braun et al. [8, 17, 18]. The plates were produced through three welding techniques: 222 FCAW specimens, 120 SAW welded specimens, and 77 LH welded specimens. The test series included different weld shapes (I-, V-, Y-, and X-grooves) and material strengths in the range from S235 (yield stress, 235 MPa) to S690 (yield stress, 690 MPa).

The weld seam geometry was scanned according to the methodology defined by Renken et al. [7] and supported by the work of Schubnell et al. [23]. A 3D laser scanner (LLT 2800–25, Micro-Epsilon) based on laser triangulation was used to capture the weld geometry. The scanner offers a spatial resolution of approximately 0.107 mm and a vertical accuracy of 0.010 mm. The acquired point cloud data were analyzed using the curvature method to accurately characterize local geometric features of the weld. For clarity in the analysis, the scanning direction, loading direction, and slice numbering are illustrated in Fig. 2.

The geometry parameters were defined as presented in [8]. Three hundred longitudinal slices (approx. 7.5 slices per mm) were obtained from the scan of each side of the specimens: top side (T) and bottom side (B). For each slice, the undercut depth (d), toe radius (r), notch angle (α), overfill (H), axial misalignment (e), and angular misalignment (φ) were determined (Fig. 3).

The geometrical factors were defined from each scanned slice, and the nomenclature is presented in the next table. The undercut depth, toe radius, and notch angle were defined at the notches on both sides of the seam weld, and therefore, the additional tag of left (L) or right (R) was added to the factor naming.

In terms of fatigue testing, there were considered only tests carried out at a temperature of 20 °C and in a range of stress ratios between −1 and 0.5. All tests were uniaxial and force-controlled in the high-cycle fatigue regime, with the applied load oriented perpendicular to the seam welds. Approximately 10% of the tests resulted in run-outs. Fatigue failure was considered to occur upon final fracture of the specimen. The run-outs were not taken into account for the statistical assessment. The axial and angular misalignment were measured before the testing through analog gauges, and the values were also registered in the dataset. In case of fracture during the testing, the fracture location was identified as the notch where the final crack propagated. Therefore, four options for fracture location were possible: top left (TL), top right (TR), bottom left (BL), and bottom right (BR) as shown in Fig. 2.

3 Data exploration

This section presents the statistical distributions of the collected weld geometry data, analyzing variations across the three different welding methods. The comparison aims to

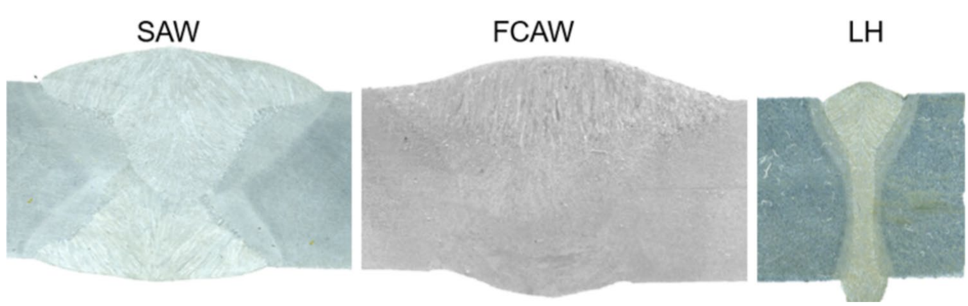

Fig. 1 Cross section of SAW, FCAW, and LH welded joints

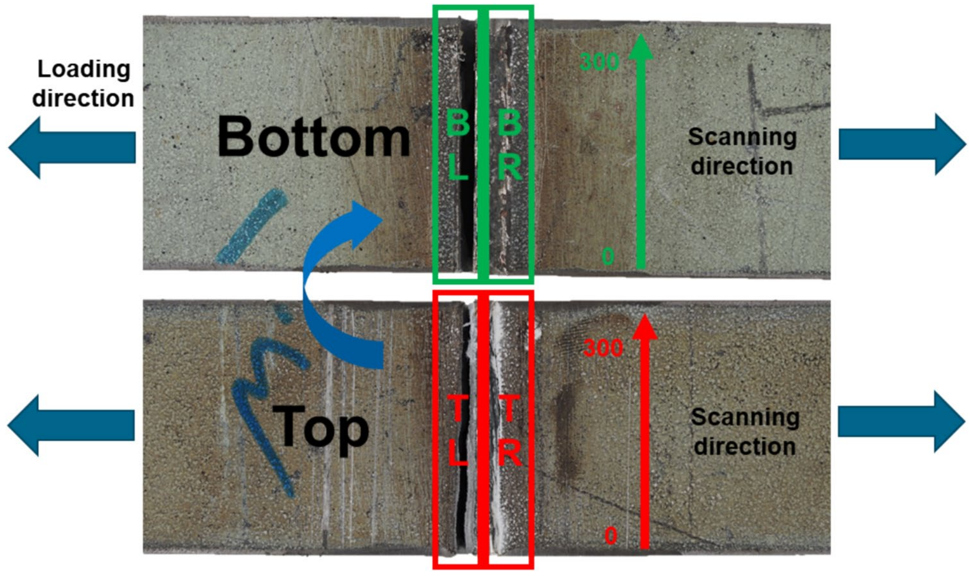

Fig. 2 Scanning orientation of the specimens and nomenclature used for notch identification

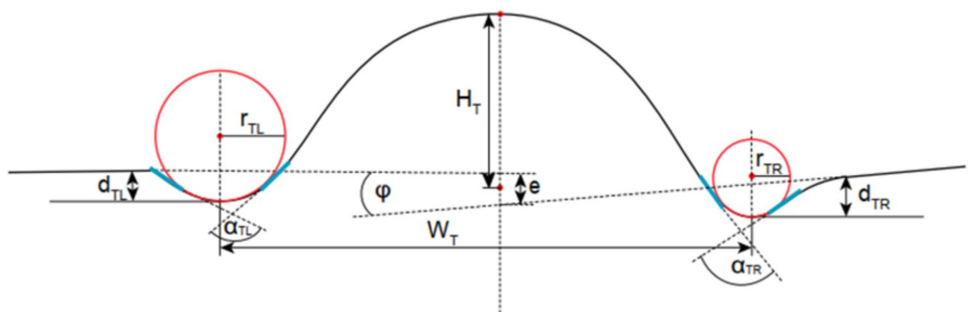

Fig. 3 Schematic representation of the top side geometry of butt-welded joints, adopted from Braun et al. [8]

identify geometric differences, their potential impact on fatigue life, and assess the quality according to ISO 5817 [9]. Additionally, similar distributions were previously reported by Braun et al. [17]. The relationship between manually measured axial and angular misalignment with the fracture location is examined.

3.1 Geometry distributions and ISO 5817 quality assessment

Figure 4 presents the top and bottom seam widths within the dataset. The LH specimens exhibit the smallest weld seam width. To analyze differences between surfaces, the data is divided into top and bottom sides, allowing for comparison with the quality limits defined in ISO 5817. Additionally, Fig. 5 presents the histograms for the three welding methods, illustrating the distribution of normalized undercut depth, ISO 5817 normalized overfill, notch angle, and toe radius within the dataset.

A visual assessment suggests that most histograms follow either a normal or lognormal distribution. However, the notch opening angle in SAW specimens distinctly exhibits a bimodal distribution [24]. In general, LH specimens show the broadest distributions across most parameters, except for the toe radius. On the other hand, SAW specimens display the sharpest distributions, while FCAW specimens exhibit an intermediate distribution range.

The undercut depth ratio to thickness distribution predominantly falls within ISO 5817 quality group B on both the top and bottom sides of the welds. Only extreme values, specifically from the LH specimens, exceed this range and are classified under quality group C. Considering the nominal undercut depth limit, 88% of the specimens in the dataset meet both requirements for quality group B. This indicates a generally high level of weld quality and highlights the influence of the welding method on undercut depth distribution and its potential impact on weld quality, especially in LH specimens that present deeper undercuts.

Similarly, the overfill height distributions predominantly fall within ISO 5817 quality group B, with peak values concentrated near the group B limit for all welding methods. However, variations exist among the different methods, particularly in the classification of extreme values. Specimens from all welding methods exhibit instances of top overfill exceeding the group B limit, with some classified under quality groups C and D. Additionally, FCAW and SAW

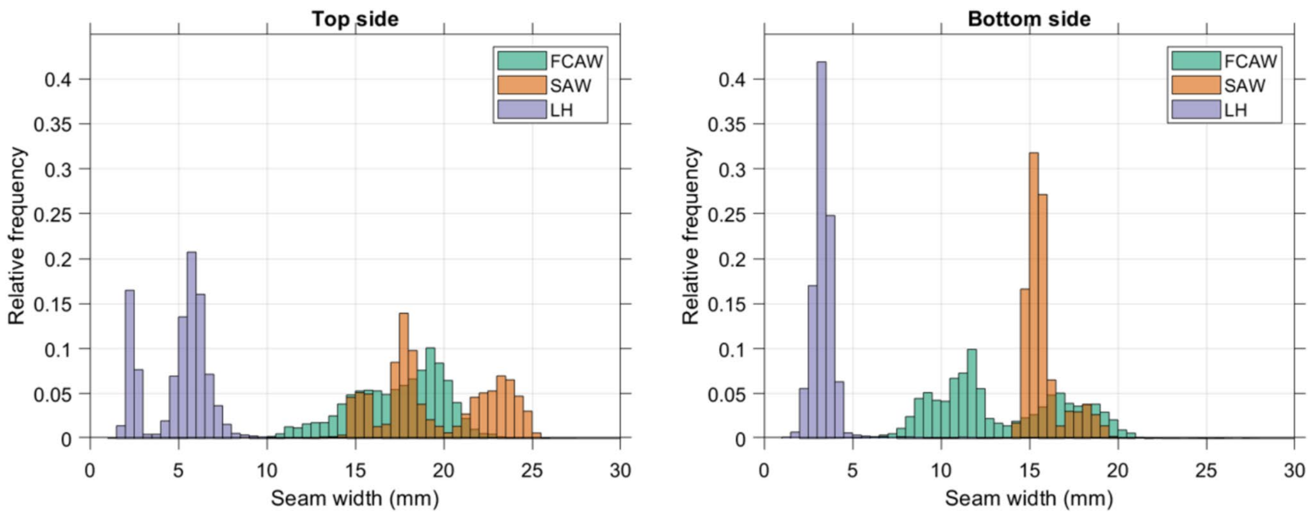

Fig. 4 Seam width histograms per welding method

specimens remain within the quality group B requirements for root overfill height; on the other hand, LH specimens exhibit higher values, placing the tail of their distribution in quality group C. Taking the overfill height limit into consideration, 79% of the specimens in the dataset satisfy both criteria required for classification within quality group B (summarized in Table 1).

The notch angle definition used in this study does not directly correspond to the flank angle limit specified in ISO 5817. However, it provides insight into the sharpness of undercuts or notches along the weld seam, which is particularly relevant due to their potential role as stress concentrators. Within the dataset, all welding methods exhibit broad distributions of notch angles, with specimens from each method displaying similarly sharp notches at the lowest end of the range.

ISO 5817 includes a toe radius limit in Annex B, establishing a relationship with expected characteristic fatigue strength categories B125, B90, and C63. In the dataset, toe radius distributions predominantly fall within the C63 group, with peak values near the transition between C63 and B90. Among the welding methods, FCAW specimens exhibit the largest toe radii, which may contribute to a higher fatigue life, as smoother notches are generally associated with lower stress concentrators [17].

A quality group according to ISO 5817 was assigned to each specimen in the dataset, based on the lowest quality observed in any scanned slice. The classification was determined using distributions of top and bottom overfill, manually measured axial and angular misalignment, and undercut depth. Overall, 202 (48%) specimens were classified in quality group B, 144 (34%) in group C, 48 (12%) in group D, and 25 (6%) were found to be out of specification (OoS). Table 1 presents a summary of the classification made according to ISO 5817.

3.2 Misalignment relation with fracture location

Figure 6 presents the manually measured axial and angular misalignment of the specimens, categorized by fracture location to evaluate potential relationships. A strong visual relationship is observed between angular misalignment and the side of fracture occurrence, particularly when the absolute angular misalignment exceeds 0.5°. In these cases, positive angular misalignments are predominantly associated with fractures initiating on the top side of the weld, whereas negative angular misalignments are more linked to fractures occurring on the bottom (root) side. A similar, though weaker, correlation is observed in the case of axial misalignment. Extreme positive or negative axial misalignments influence whether the fracture initiates from the left or right notch.

A positive angular misalignment is expected to introduce secondary bending stresses on the top side and compression stresses on the weld root (bottom). On the other hand, negative angular misalignments produce additional tensile stresses on the bottom side and compression stresses on the top side. These additional stresses have two origins: (1) induced during the clamping by forcing the alignment (constant stress during fatigue testing) and (2) induced by the test loading (time-dependent stresses that interact with existing misalignment-induced effects) [26]. In the lower angular misalignment range (–0.5° to 0.5°), 31% of the specimens failed on the compressively stressed side. In contrast, within the higher angular misalignment range (–3.0° to –0.5° and 0.5° to 3.0°), 99% of the specimens failed on the tensile-stressed side.

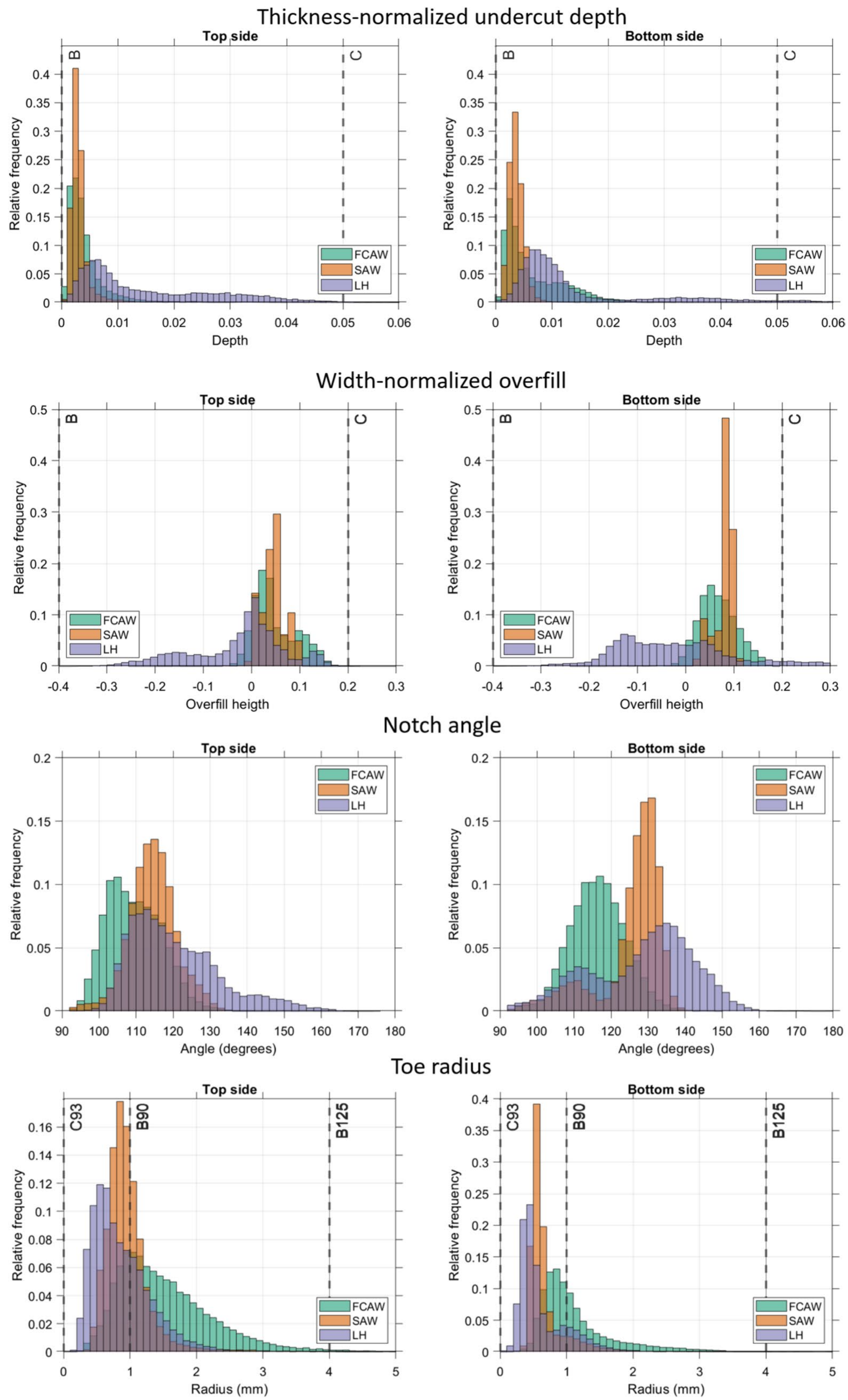

Fig. 5 Histograms of weld geometry parameters distinguished between different welding methods and comparison with ISO 5817 quality groups

Table 1 Summary of quality classification according to ISO 5817

Welding method	Group B	Group C	Group D	Group OoS
Undercut depth				
FCAW	212 (95%)	0 (0%)	8 (4%)	2 (1%)
SAW	108 (90%)	0 (0%)	11 (9%)	1 (1%)
LH	51 (66%)	15 (20%)	10 (13%)	1 (1%)
All specimens	371 (88%)	15 (4%)	29 (7%)	4 (1%)
Overfill height				
FCAW	163 (73%)	46 (21%)	13 (6%)	0 (0%)
SAW	113 (94%)	4 (3%)	1 (1%)	2 (2%)
LH	56 (72%)	12 (15%)	9 (12%)	0 (0%)
All specimens	332 (79%)	62 (15%)	23 (5%)	2 (1%)
Axial misalignment				
FCAW	221 (99.5%)	1 (0.5%)	0 (0%)	0 (0%)
SAW	120 (0%)	0 (0%)	0 (0%)	0 (0%)
LH	77 (100%)	0 (0%)	0 (0%)	0 (0%)
All specimens	418 (99.8%)	1 (0.2%)	0 (0%)	0 (0%)
Angular misalignment				
FCAW	167 (75%)	55 (25%)	0 (0%)	0 (0%)
SAW	52 (43%)	47 (39%)	0 (0%)	21 (18%)
LH	77 (100%)	0 (0%)	0 (0%)	0 (0%)
All specimens	296 (71%)	102 (24%)	0 (0%)	21 (5%)
Assigned quality				
FCAW	123 (55%)	76 (34%)	21 (9%)	2 (2%)
SAW	41 (34%)	45 (38%)	12 (10%)	22 (18%)
LH	38 (49%)	23 (30%)	15 (20%)	1 (1%)
All specimens	202 (48%)	144 (34%)	48 (12%)	25 (6%)

According to the observed behavior, angular misalignment in moderate or high misaligned specimens may determine which stress concentrators are more likely to initiate the failure crack. Rather than always favoring the highest stress concentrator in the specimen, crack initiation is more likely to occur at the most significant concentrator located on the tensile-stressed side, although there might be a sharper notch at the other side.

4 Statistical assessment of influencing factors

This section studies the correlation between various geometric factors presented in the previous section and the fatigue strength of butt-welded specimens. First, the stress range obtained from the fatigue tests is adjusted using the stress magnification factor due to misalignment-induced secondary bending stresses. The impact of this correction is evaluated by examining changes in the scatter of the test results. Next, a linear regression model is fitted to the logarithm of the number of cycles to failure (Nf) and the corresponding stress range (ΔS) for each welding method test data. Before assessing the relationship between residuals and the weld geometric factors, the normality of the residual's distribution is examined to ensure the validity of the analysis.

Stress ranges were corrected and merged according to IIW recommendations to minimize loading effects and focus on the role of weld geometry. Separate analyses of the stress

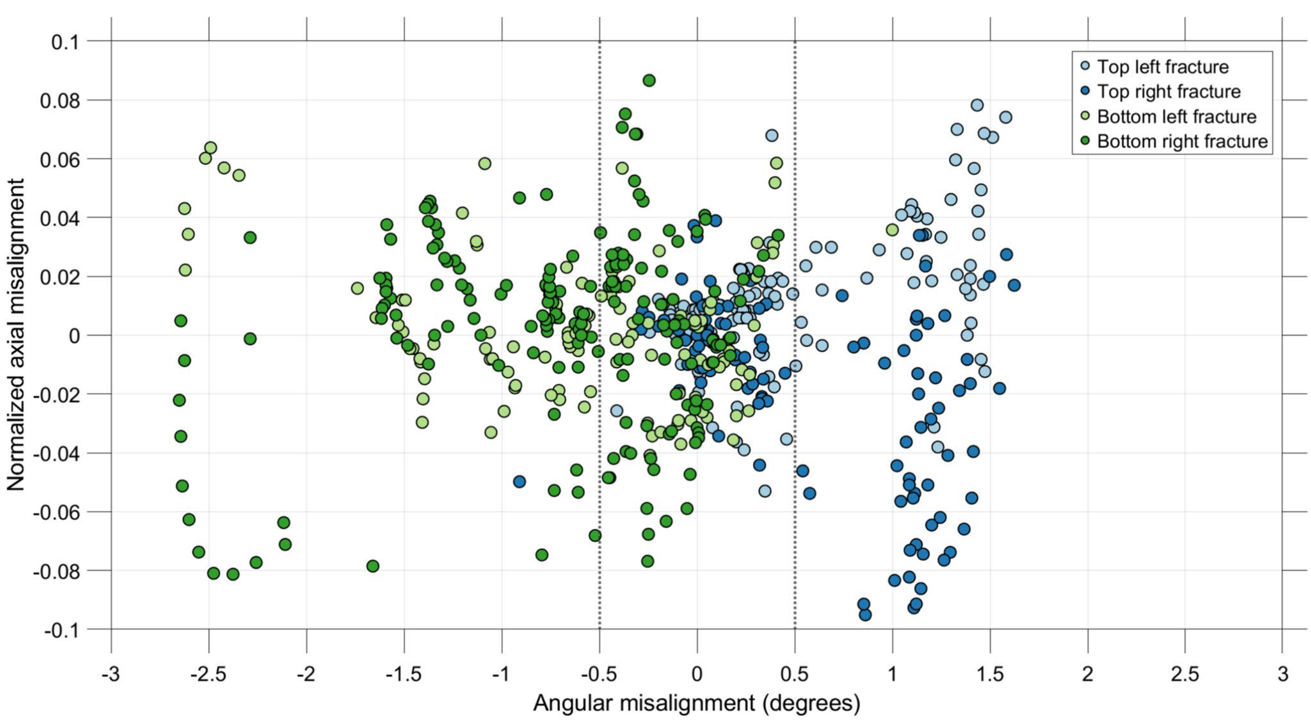

Fig. 6 Specimen axial and angular misalignments segmented by fracture location

ratio groups showed no significant differences. Since only a small number of tests were fully reversed ($R<0$), most of the data corresponded to tensile loading ($R>0$). Statistical checks confirmed that the corrected fatigue life data follow a normal distribution, allowing all results to be analyzed together. These findings indicate that weld geometry effects on fatigue life are independent of stress ratio, since local stress concentration is controlled by geometry.

4.1 Stress range misalignment correction

The stress range was corrected using the stress magnification factor according to the IIW recommendations [15, 25]. This allows for the correction of the secondary bending stress induced by the axial and angular misalignment and to focus on the effects of the local weld geometry on the fatigue life, since the misalignments affect the whole specimen. A stress magnification factor was computed for each scanned slice in the dataset. To determine a representative statistical value, a stress magnification factor was calculated for each scanned slice, and then different statistical measures were used to correct the testing stress range, including the mean, median, mode, and quantiles ranging from 0 to 100% of the stress magnification factor distribution.

Each specimens stress range was thus multiplied by the stress magnification factors calculated. The selection of the magnification factor was guided by the criterion of minimizing the scatter coefficient (T_S) adopted from DVS [26, 27]. Briefly, the scatter coefficient was defined as the ratio between the stress range with 10% and 90% survival probability at $2{\cdot}10^6$ cycles:

$$T_S = \frac{\Delta\sigma_{10\%}}{\Delta\sigma_{90\%}}$$

The scatter calculated for each quantile is plotted in the Fig 7. It can be observed that applying the stress magnification factor using manually measured misalignments or the mean value resulted in the lowest scatter coefficients. Based on the scatter values, the manual measurements of misalignment were selected for stress range correction and subsequent correlation analysis.

4.2 Fatigue life per quality group

As first instance, a quality class was determined for each tested specimen in order to study the relation between the weld quality according to ISO 5817 and the fatigue life. The quality class was selected using the lowest quality geometric parameter found in any slice of the specimen. The weld overfills, undercut depth, axial misalignment, and angular misalignment were considered to define the quality class for each specimen. For angular misalignment, the limits were adopted from Annex B of ISO 5817. Forty-eight percent of the specimens were classified as B class, 34% C class, 12% D class, and 6% out of the specifications (OoS) as summarized in Table 1. The fatigue test S-N curve with the corresponding quality group is shown in the Fig 8 together with the characteristic fatigue strength obtained for each class calculated at a fixed slope $m=3$ following the IIW recommendations.

Visually, it can be noted that there is no clear location or region in the S-N where one of the quality groups has a greater presence. Therefore, it can be clearly interpreted that producing a specimen in a determined quality does not assure a given fatigue performance. However, the statistical determination of the characteristic fatigue strength for each class group showed low difference between the C, D, and OoS groups. The minimum strength calculated for these groups (87 MPa) is

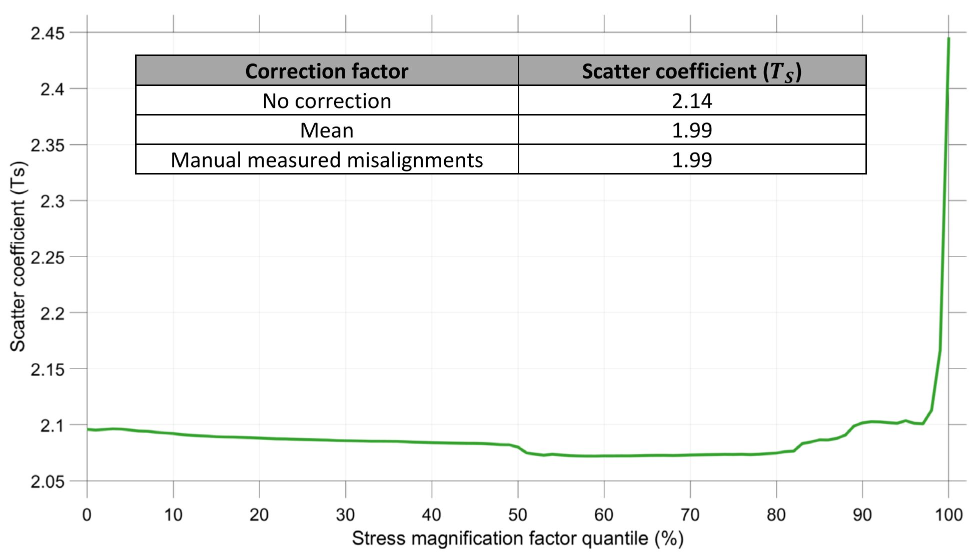

Correction factor	Scatter coefficient (T_S)
No correction	2.14
Mean	1.99
Manual measured misalignments	1.99

Fig. 7 Scatter coefficient (T_S) for different stress magnification corrections and summary of scatter results obtained

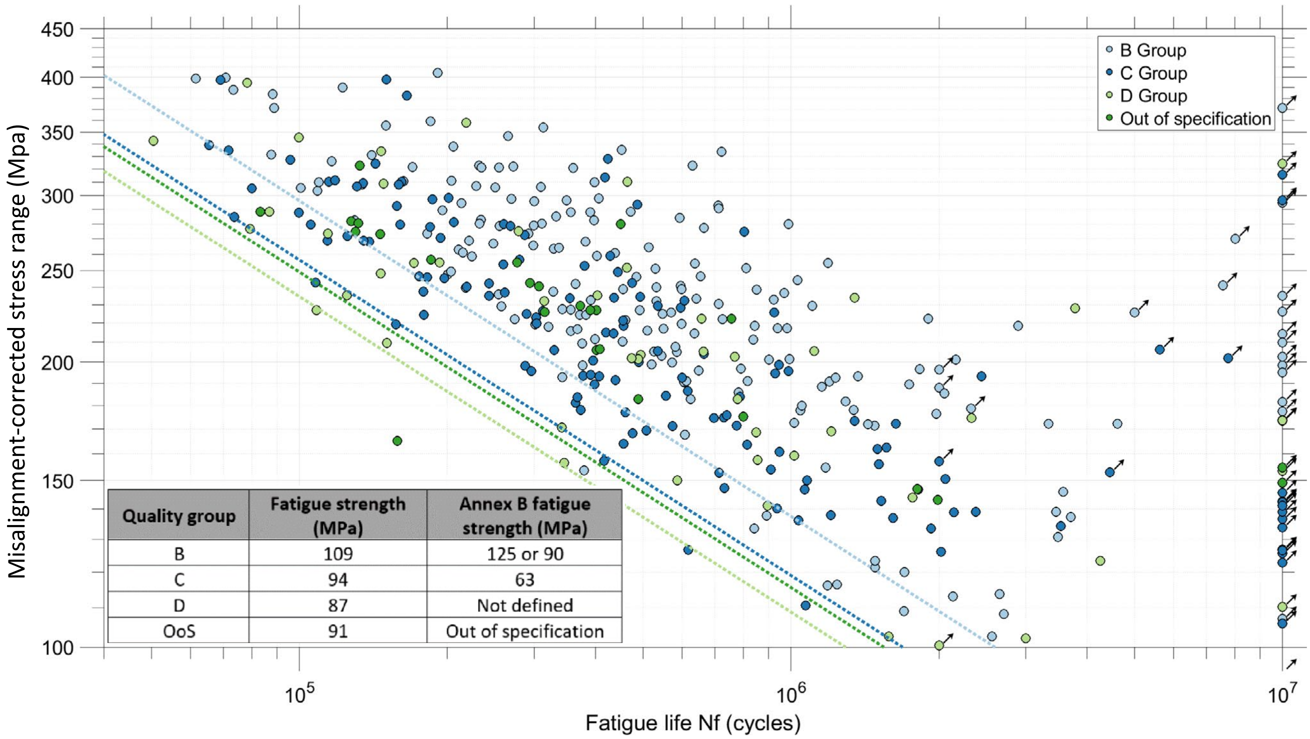

Fig. 8 Characteristic fatigue strength per ISO 5817 quality group (arrows indicate run-out specimens) calculated using the misalignment corrected stress range

40% higher than the 63 MPa proposed normative value in Annex B of ISO 5817 for the C group. On the other hand, the 109 MPa estimated for the B class group can be found as an intermediate value between the 125 MPa and 90 MPa proposed in Annex B.

4.3 Regression model and statistical assessment

To assess the effect of the local geometric factors on the fatigue strength of the butt-welded joints, a statistical assessment of the corrected test results is performed. Correlations between the number of cycles to failure (N_f) and the quantiles of the geometric distributions are determined to quantify the impact on fatigue strength and identify the most representative quantile describing this relationship. The fatigue tests ranging from the number of cycles to failure between 5.10^4 and 1.10^6 were considered. Specimens were grouped by welding method to limit the influence of process-related effects (differences in HAZ, microstructures, and residual stresses). Given their small size, specimens are expected to have low residual stresses. All specimens were also analyzed together to evaluate the general applicability of the correlations.

The methodology chosen to estimate the correlation was previously applied by Braun et al. to correlate fatigue test results with temperature and non-geometrical parameters [21]. Consequently, a linear regression model (assuming a normal distribution) was fitted to the logarithm of the number of cycles to failure and stress range of the selected data. Then, the residual of each data point was calculated considering the stress range as the independent variable and the number of cycles to failure as the dependent variable, as illustrated in Fig. 9. The residuals between test data and the regression model are used to determine the correlation coefficients in the next section.

In Fig. 10, residuals are visually compared with the fitted logarithmic number of cycles to failure and assessed by an Anderson-Darling (AD) test to verify the assumption of normally distributed residuals [28]. The null hypothesis of the Anderson-Darling (AD) test states that the data originates from a population following a normal distribution. This is assessed by calculating the test statistic value AD and comparing it to a critical (tabulated) value AD^* at a chosen significance level, in this case, 0.05. The Anderson-Darling test was applied as it has been used in previous studies to verify the assumption of normally distributed fatigue test data, since it shows higher sensitivity to extreme values compared to other normality tests [22, 29].

The visual assessments show a symmetrical function that could be part of a normal distribution. Moreover, the result is supported by the AD test results as the selected data set's AD value is smaller than the critical value AD^*. Therefore,

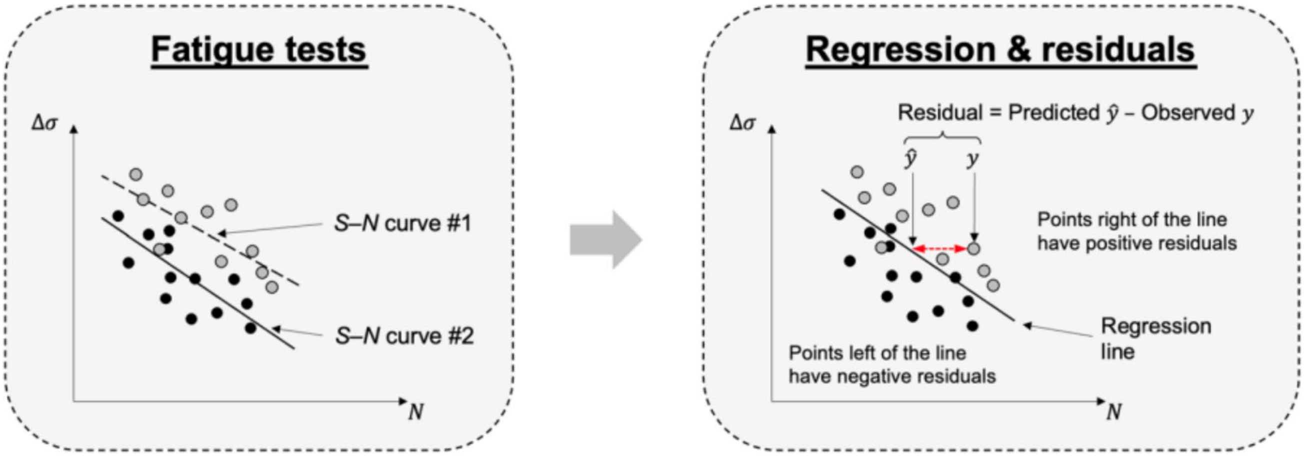

Fig. 9 Linear regression fitting to the fatigue tests results and residuals determination, adapted from Braun et al. [22]

it can be assumed that the filtered fatigue test data is log-normally distributed. Then, the deviation of each data point (residual) from the expected fatigue life at a given stress range (fitted S-N curve) can be examined against the geometric parameters to identify possible relations.

4.4 Fatigue life and weld geometry correlation

The correlation between the residuals of the logarithmic number of cycles to failure and the scanned geometrical parameters was analyzed. In order to do this, the Spearman correlation coefficients are calculated to assess relations between the variables. The coefficients were calculated for the following geometric parameters: undercut depth, normalized overfill, overfill as defined in ISO 5817, notch angle, toe radius, axial, and angular misalignment.

A Spearman-type correlation, which measures the rank-correlation and direction of a monotonic relationship between two variables, was chosen for the analysis. This approach is particularly relevant in the context of weld geometry and fatigue strength, as stress concentration factors in the literature are typically governed by nonlinear functions of the weld geometry parameters. Although only Spearman correlations are presented, additional tests with Pearson correlations revealed no significant differences, indicating that the relationships are partly linear and that the nonlinearities in the data are not pronounced. Therefore, the choice of correlation method has little effect on the overall assessment of associations between weld geometry and fatigue life. Previous studies have also applied Spearman correlations to investigate the link between weld geometry and fatigue life in order to capture potential nonlinear effects; Tang et al. similarly reported slight differences between Pearson and Spearman results [30, 31].

Additionally, for undercut depth, overfill, notch angle, and toe radius, separate analyses were conducted using datasets that included only top-side or bottom-side, only fracture side, and only the fracture notch values. These subsets were added to study interactions between local geometry from the fracture side and notch with the fatigue life, which might show stronger correlations due to the misalignment induced stresses, as observed in Fig. 6. Table 2 provides the mathematical definitions of the geometrical parameters per slice, which were used to compute the statistical distributions for each scanned specimen. To evaluate the influence of each geometric parameter on fatigue life, statistical descriptors including minimum, maximum, and quantiles (ranging from 0 to 100% in 1% increments) were calculated for each parameter. This approach allows for a comprehensive assessment of which statistical representation best captures the relationship between weld geometry and fatigue life.

Figure 11 presents the results obtained from the correlation analysis for normalized overfill height for each welding method. According to Ratner, a correlation can be considered weak, moderate, and strong respectively, with the correlation value [32]:

- Between 0 and 0.3 (0 and −0.3) indicate a weak positive (or negative) relationship
- Between 0.3 and 0.7 (0.3 and −0.7) indicate a moderate positive (or negative) relationship
- Between 0.7 and 1.0 (−0.7 and −1.0) indicate a strong positive (or negative) relationship

It can be observed that the overfill on both sides exhibits the highest correlation with fatigue life at lower quantiles. Although the strength of this correlation is only moderately negative, it can be generalized for all the welding methods.

Fig. 10 Residuals from linear regression model (left) and the normal probability plot of residuals with the results of the Anderson-Darling test (right)

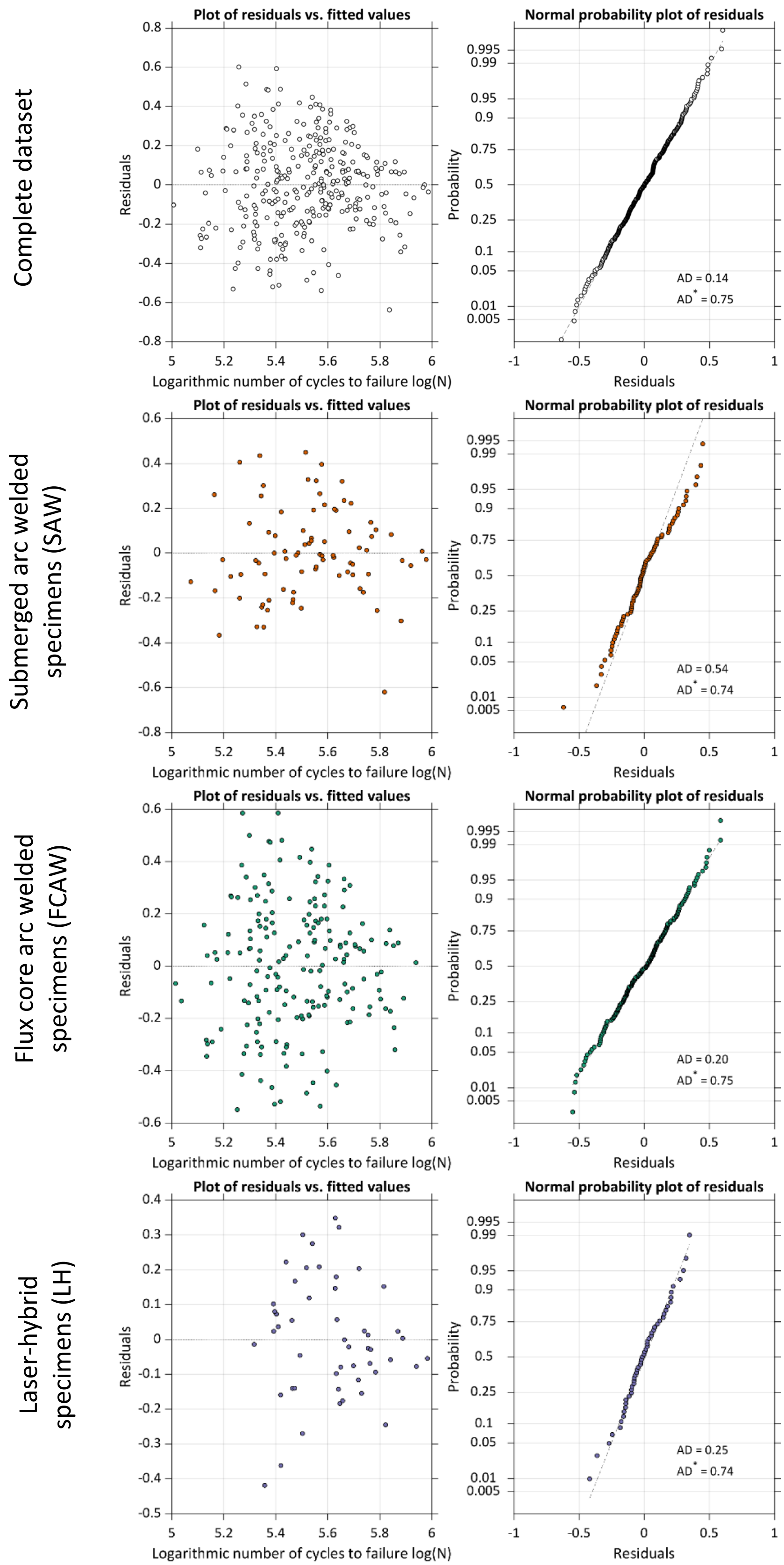

In contrast, the subsets of data limited to the top side, bottom side, or fracture side show weaker correlations, suggesting that using all available overfill data provides a more accurate representation of its relationship with fatigue life. Comparable, barely moderate negative correlations are also observed in the FCAW and SAW specimen datasets.

For the LH specimens, fatigue life is influenced by the overfill on the top side, showing a constant and strong negative correlation across nearly all quantiles. On the other hand, lower correlations are found at the minimum or lower quantiles, while the maximum quantiles do not exhibit even stronger correlations. This pattern suggests that it is the overall condition of the overfill, rather than extreme values, that has a more significant impact on LH fatigue life. Furthermore, the opposite behavior can be observed between LH bottom overfill and fatigue life, where a positive moderate correlation is present at low quantiles.

Figure 12 presents the results obtained from the correlation analysis for normalized undercut depth for each welding method studied. No moderate or strong correlations between undercut depth and fatigue life are observed in the SAW specimens. In contrast, the FCAW specimens exhibit a weak but unexpected positive correlation at higher quantile values on both sides, though this finding

Table 2 Geometrical parameters definition per slice

Name	Geometrical factor normalization per slice
Top undercut depth	Maximum between d_{TL}/t_L and d_{TR}/t_R
Bottom undercut depth	Maximum between d_{BL}/t_L and d_{BR}/t_R
Top overfill	H_T/W_T
Bottom overfill	H_B/W_B
Top notch angle	Minimum between α_{TL} and α_{TR}
Bottom notch angle	Minimum between α_{BL} and α_{BR}
Top toe radius	Minimum between r_{TL} and r_{TR}
Bottom toe radius	Minimum between r_{BL} and r_{BR}
Axial misalignment	e/minimum between t_L and t_R
Angular misalignment	Absolut value from Φ

may lack significance. When analyzing the entire dataset, no consistent or generalizable correlation between undercut depth and fatigue life can be identified.

The LH specimens display a moderate negative correlation at lower quantiles, suggesting that the shallowest undercuts may be indicative of the overall undercut condition of the seam. Additionally, an increasing trend in correlation is observed toward higher quantiles, implying that deeper undercuts also contribute significantly to reduced fatigue life. Although this trend is present across all datasets, the

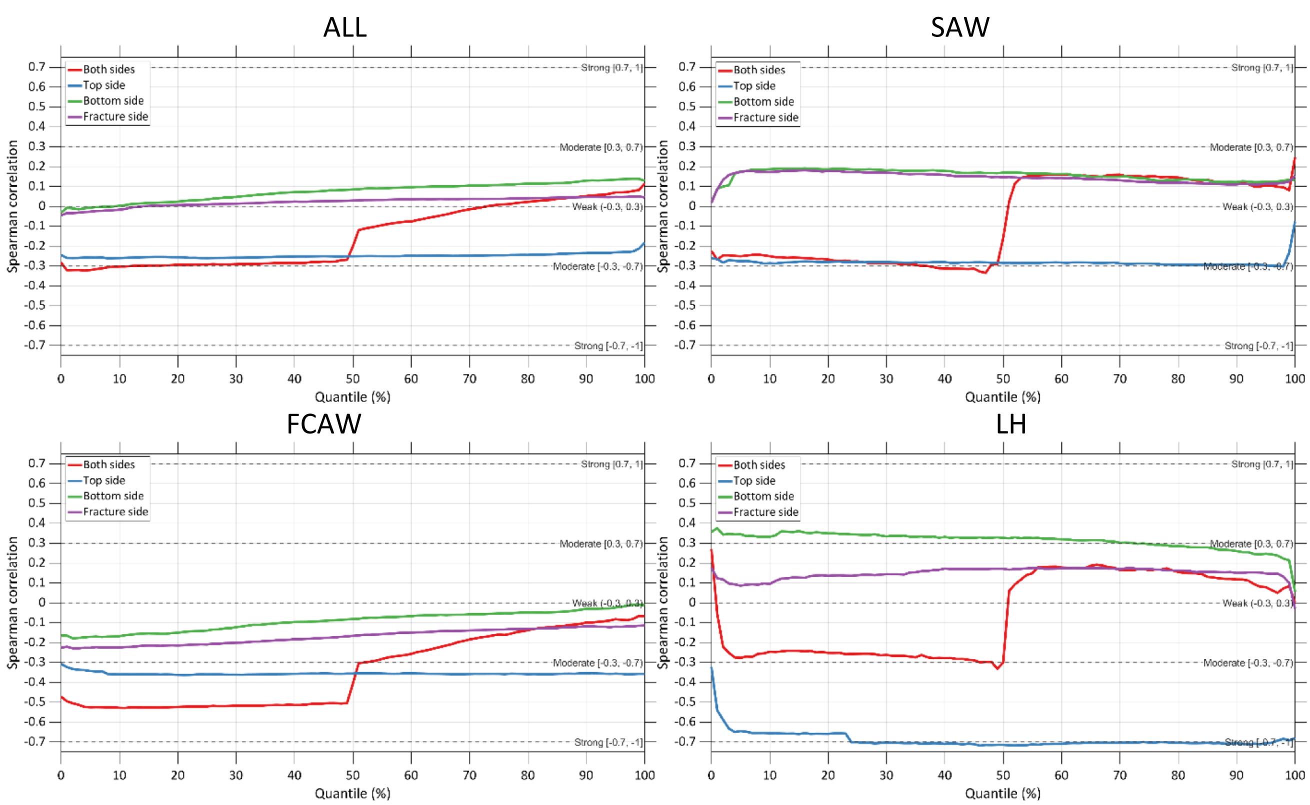

Fig. 11 Normalized overfill height correlation plots

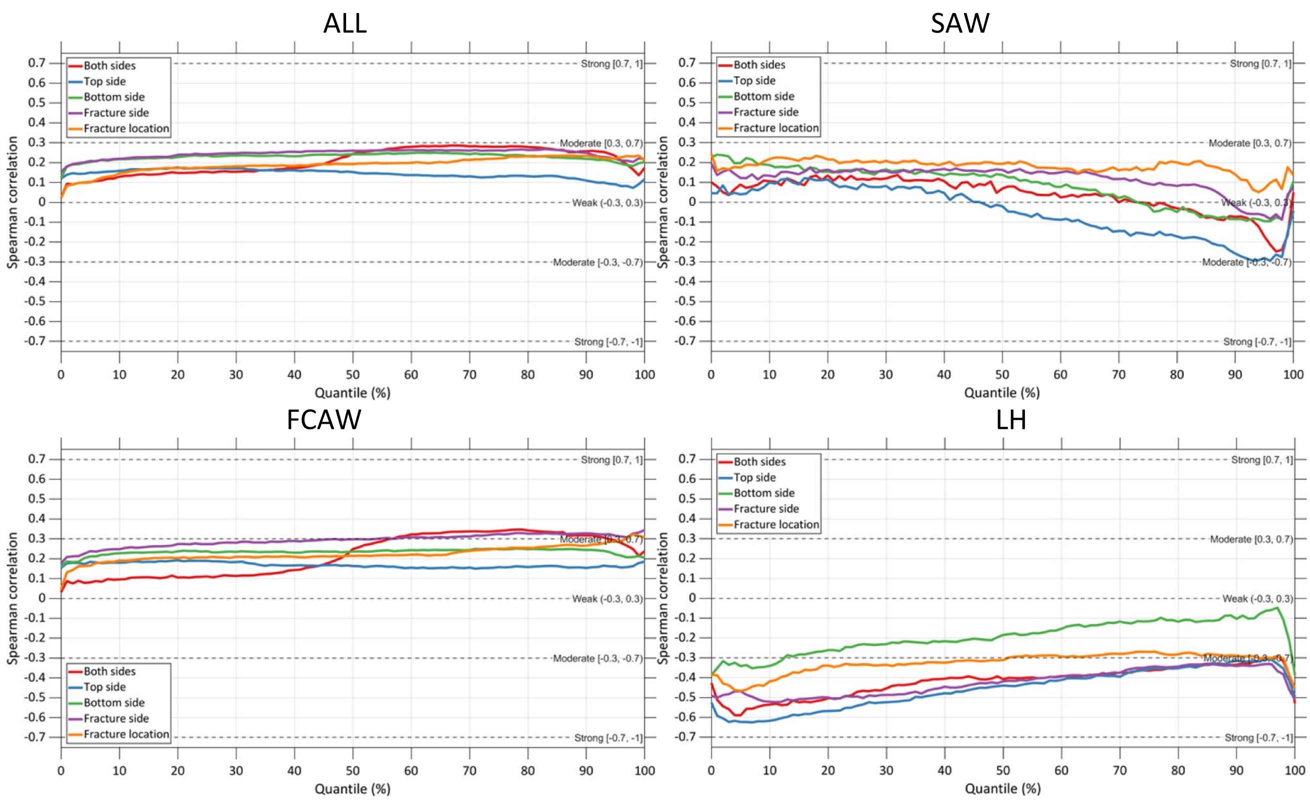

Fig. 12 Normalized undercut depth correlation plots

correlations remain relatively weak. Overall, the results suggest that extreme undercut values (either shallow or deep) correlate better with changes in the fatigue performance of LH welds. Only a few specimens showed noticeable undercuts; therefore, the data might not be sufficient to come to a clear conclusion regarding the undercut effect on fatigue life.

Figure 13 presents the results obtained from the correlation analysis for notch angle for each welding method studied. When considering the notch angle from all specimens collectively, no moderate correlation is observed. However, when analyzing by welding method, SAW specimens exhibit a moderate positive correlation, particularly when considering both sides and the bottom side datasets. This suggests that larger notch angles may contribute to improved fatigue performance in SAW welded joints, as expected from a structural mechanic point of view. On the other hand, for FCAW specimens, a moderate negative correlation is observed at lower quantiles on both sides and along all the quantile range on the top side, indicating that more opened notches may be associated with reduced fatigue life in these specimens. This unexpected behavior might be related to different microstructural properties originated from the welding method.

LH specimens display both trends, with a negative correlation between fatigue life and notch angle on the top side and a positive correlation on the bottom side. This pattern reflects the general behavior observed across all welding methods: top side measurements tend to show negative correlations, while bottom side values often show positive correlations. Furthermore, an increasing negative correlation between fracture location and the maximum notch angle was observed in LH specimens. This suggests that extreme values of the notch angle not only influence where the crack initiates, but also have a significant impact on the overall fatigue life.

Figure 14 presents the results obtained from the correlation analysis for toe radius for each welding method studied. No significant relationship is observed when evaluating the correlation between toe radius and fatigue life across the complete dataset. SAW specimens show a moderate negative correlation on the top side, particularly at the extreme low quantiles. FCAW specimens exhibit moderate correlations between top side toe radius and fatigue life. Similarly, LH specimens reveal a moderate positive correlation on the top side, suggesting that larger toe radii (smoother transitions) increase the fatigue resistance.

Additionally, the Spearman correlation results for manually measured misalignments are presented in Table3, and no moderate or strong relation can be observed. Therefore, this result could verify that the misalignment correction

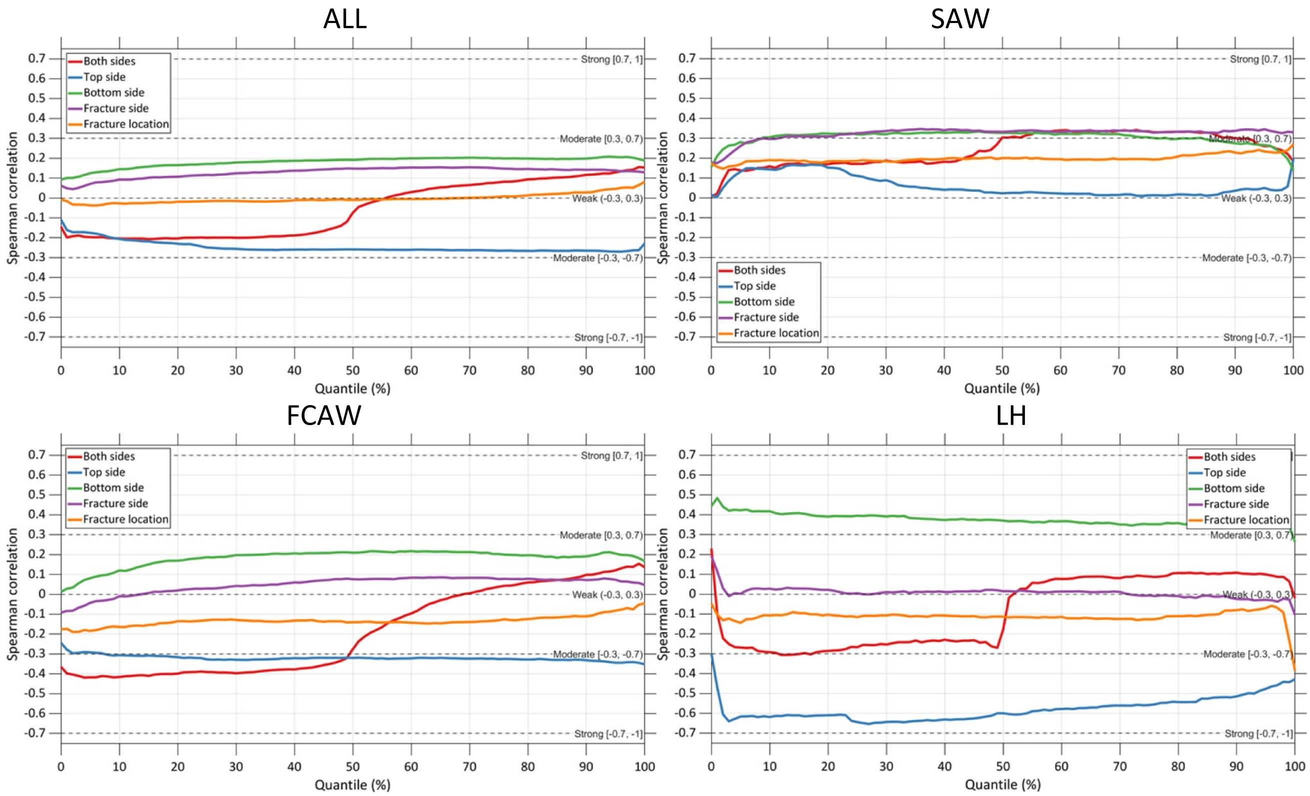

Fig. 13 Notch angle correlation plots

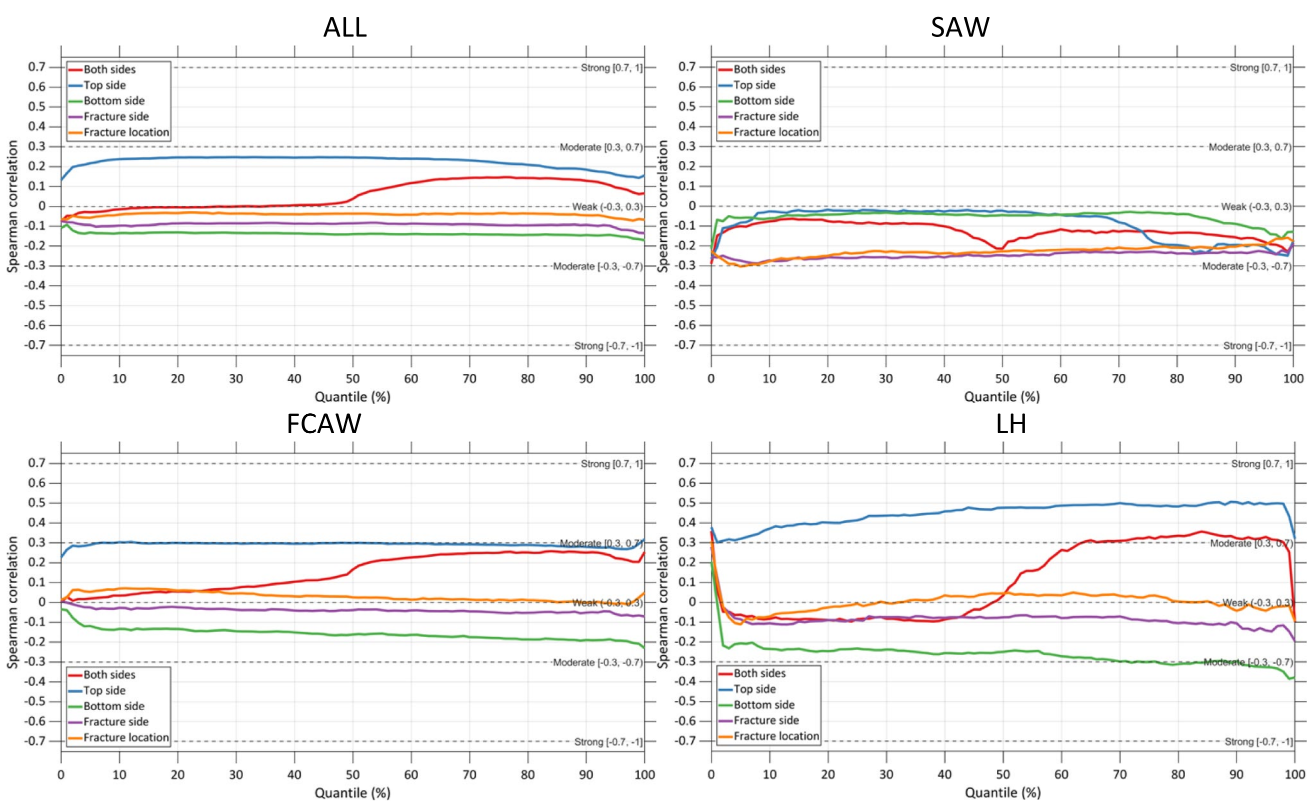

Fig. 14 Toe radius correlation plots

Table 3 Spearman correlation between misalignments and fatigue life

Dataset	Normalized axial misalignment	Angular misalignment
Complete dataset	−0.02	0.08
SAW	0.14	−0.12
FCAW	−0.07	0.20
LH	−0.27	0.25

due to secondary stresses was successful. However, it is important to note that the stress range was corrected according to the IIW recommendations, which should mitigate the influence of misalignments on fatigue life.

5 Discussion

The statistical evaluation of the weld geometry parameters and their influence on the fatigue strength from the previous section showed that the fatigue life is influenced by a combination of local geometrical parameters, with distinct trends depending on the welding method used.

5.1 Influence of misalignments

The analysis of the manual measured misalignment relation with the fracture location showed the decisive role of angular misalignment in determining the fracture initiation side. It was observed that specimens with higher angular misalignments exhibited a clear tendency for crack initiation on the tensile-stressed side (99% of fractures occurring there when misalignment exceeded ± 0.5°). However, neither the notch geometry nor the fracture side itself showed stronger correlations with fatigue life in the Sect. 4 correlation analysis. This suggests that while angular misalignment acts as a deciding factor for the initiation point of the crack, the local geometry of the additionally tensile-stressed notch is not conclusive in defining the fatigue life. Therefore, once initiated, the fatigue crack growth appears to be governed by other factors rather than the initial geometric initiator. This highlights the importance of studying other secondary influences like the metallurgical notch or residual stresses [22].

Moreover, the choice of quantile used for the stress magnification factor correction had a minor impact on the scatter of the fatigue test data. In the literature, Niraula et al. calculated the stress magnification factor according to the IIW recommendations using the average of the angular and axial misalignments of each scanned specimen distribution [15]. Among the approaches evaluated, correcting the stress range using the manually measured misalignment and applying the distribution mean value resulted in the lowest scatters. This suggests that manual measurement (simpler and practical) could be sufficient in the case of fatigue test specimens. However, this method might not be as reliable in the case of full-sized structures. This is attributed to the origin of the misalignment; rather than being a local geometric feature, it tends to remain relatively uniform along the specimen since they are caused by initial plate positioning during welding.

5.2 Quality classes and fatigue performance

The findings of this study are consistent with those reported by Glienke et al., who showed that SAW joints meeting ISO 5817 quality level B can be classified within FAT class 100 [10]. The current results suggest that this classification may be extended to FCAW and LH joints as well. In the present analysis, high-quality welds exhibited approximately 15% higher characteristic fatigue strength compared to the lower-quality specimens. However, the observed increase between levels was less than the 30% difference typically expected between classes C63 and B90 from ISO 5817 (calculated from the values presented in Fig. 8). It might be taken into account that the works from Hobbacher and Kassner used to develop the FAT classes were developed using linear fracture mechanics on 10-mm-thick butt-welded joints [11]. In the present study, joints between 6 and 20 mm were employed; therefore, Annex B might be representative for thicker specimens.

The lowest quality groups exhibited similar fatigue strengths, indicating that the classification system could potentially be simplified into two broader categories based on local geometry: high-quality joints (equivalent to Class B) and low-quality joints (combining Classes C and D). High-quality welds present a characteristic fatigue strength of around 110 MPa, while lower-quality joints have a fatigue strength of around 90 MPa. This suggests that the current ISO 5817 classification may underestimate the fatigue performance of poorer-quality welds.

5.3 Influence of the overfill

The normalized overfill was found to be the only geometric parameter showing consistent correlation with fatigue performance across all welding methods analyzed. This parameter, defined as the weld height normalized by the weld width, serves also as an indirect indicator of the flank angle, reflecting the steepness of the cross-sectional transition created by the weld seam. When interpreting normalized overfill as flank angle, the trends observed align well with previous findings reported by Schubnell et al. [12], Glienke et al. [10], Braun et al. [18], and Schork et al. [16], which supplementary examined GMAW, TIG, and MAG welded specimens [6, 10, 18]. As a result, both overfill and flank angle may be considered generalizable indicators for fatigue behavior across a wide range of welding methods.

From a practical standpoint, this implies that focusing on controlling weld overfill could be a common strategy in improving fatigue performance in any weld structures as presented in ISO 5817.

5.4 Influence of undercut

No moderate influence of undercut depth on fatigue life was observed in SAW specimens individually or in the complete dataset. In the case of FCAW specimens, a weak positive correlation appeared at high quantiles using both-side data, which is unexpected compared with the literature. This may suggest that undercut depth, in this context, acts as a proxy for another parameter, and it is also important to consider that FCAW specimens showed a relatively narrow range of undercut values, with depths typically less than 1% of the plate thickness, which might limit the observation of undercuts decreasing the fatigue life. SAW specimens also exhibited undercuts mostly below 1% of thickness, which may explain the lack of moderate correlations in these specimens. Similar results were obtained by Schubnell et al. while applying the IBESS approach to butt welds from various welding methods, where no correlation with undercuts was reported [12].

For LH joints, two observations can be made. First, they displayed a wider undercut distribution, reaching up to 5% of thickness. Secondly, they showed their highest sensitivity to undercut depth on the top side, particularly in the lower quantile range, suggesting that shallow undercuts may be representative of overall weld quality. A moderate negative correlation was also observed when considering both sides or the bottom side. Thus, using a 5% quantile from both surfaces' distribution may provide a suitable metric for characterizing undercut influence in LH specimens. The second observation is that LH specimens are sensitive to maximum undercut depth values; therefore, the effects of the undercut on fatigue life might be evaluated both through an overall statistical metric and through the maximum observed value. Regarding this topic, Niraula et al. have found in LH specimens that the undercut average depth was an indicator of fatigue strength; this study shows that using low quantiles for this assessment might produce better results [15].

In general, undercut depths less than 1% of the specimen thickness show minimal influence on fatigue life across all welding methods. However, larger and more variable undercuts (as found in LH specimens) can play a significant role and justify the continued use of maximum depth criteria such as those defined in ISO 5817 [9].

5.5 Influence of notch angle

No consistent correlation was observed across all welding methods. However, analyzing each welding process individually revealed moderate correlations between notch angle and fatigue life. This suggests that the differing effects across methods cancel out one another in the combined analysis. Therefore, the effect of the notch angle on fatigue life cannot be generalized for any welding method. SAW specimens exhibited a moderate positive correlation in the higher quantile range (60% to 85%) using both sides of the weld. In contrast, FCAW joints showed a moderate negative correlation in the lower quantile range (5% to 40%), especially on the top side. These findings insinuate potential interactions between notch angle and other weld-related variables.

LH specimens presented another contradictory behavior: a moderate negative correlation with top side notch angle, and a moderate positive correlation on the bottom side. Similar tendencies appeared in SAW and FCAW specimens, although with weaker correlation strength.

Furthermore, direct comparison with existing literature is difficult due to the specific definition of notch angle used in the present dataset. In specimens with a defined undercut, the notch angle effectively captures the degree of notch openness, which is relevant to local stress concentration and fatigue performance. However, in regions without a distinct undercut, the notch angle may exhibit instability.

5.6 Influence of toe radius

No significant correlation was identified between fatigue life and toe radius across all welding methods. Likewise, SAW specimens showed no notable correlation. FCAW specimens, however, exhibited a moderate positive correlation with the top side toe radius, largely independent of the selected quantile metric. A similar trend was observed in LH specimens, though the most representative correlation was found at higher quantiles. Additionally, for LH joints, a moderate negative correlation was also noted on the bottom side, which could be particularly useful for evaluations limited to a single accessible surface.

These results align partially with findings from Schork et al., which reported similar toe radius effects in TIG and MAG welded joints [6]. However, Schubnell et al., in more recent work analyzing scanned seam welds across different welding techniques (which contained data from the present dataset), did not identify strong correlations with toe radius [12]. This shows that the influence of toe radius may be context-dependent and sensitive to welding methodology.

6 Conclusion

This study evaluated systematically the relationship between weld local geometry and the fatigue life of scanned butt-welded joints fabricated using SAW, FCAW, and LH welding methods. The following conclusions can be drawn from the investigation:

- Stress correction using the manually measured misalignment produced the lowest scatter in fatigue data. This result shows that simplified manual measurements may be sufficient for practical applications.
- The characteristic fatigue strength of high-quality specimens (ISO 5817 B class) was approximately 15% higher than that of lower-quality groups, which performed similarly to each other. This suggests that current ISO classifications may underestimate the fatigue resistance of lower-quality welds and that a two-tier classification (high and low quality) may be appropriate.
- Overfill emerged as the only geometric parameter correlated with fatigue life across all welding methods, reinforcing its relevance for weld quality assessment.
- LH specimens are more sensitive to variations in the local weld geometry.
- The highest correlations were generally observed at specific low or high quantiles rather than at central tendencies, highlighting the importance of full-distribution analysis rather than relying on mean values.

The results of this study highlight the potential of using the geometry parameters low or high quantiles to obtain representative stress concentrator factors to use in fitness for service assessments. Integrating scan-based geometry analysis into inspection and manufacturing of structures could lead to more accurate fatigue life predictions and improved structural reliability. Further work should extend these findings and study their interactions with residual stresses and microstructural properties. Moreover, the findings could be integrated with machine learning models to rapidly estimate fatigue life for new joints, enabling practical and efficient extrapolation to complex welded structures after scanning weld geometries.

Author contributions Martin Leonel Melucci: writing—original draft, visualization, validation, conceptualization, software, investigation, and formal analysis. Sulaiman Shojai: review and editing, conceptualization, and supervision. Mahamudul Hasan Tanvir: conceptualization and data curation. Moritz Braun: writing—review and editing, methodology, conceptualization, and supervision.

Funding Open Access funding enabled and organized by Projekt DEAL. The work was performed within the research project WeldScanPro—“Development of an approach for inline inspection and analysis of welded joints in offshore wind turbines based on optical measurement methods and artificial neural networks” funded by the German Federal Ministry for Economic Affairs and Energy (project number 03SX595B).

Gefördert durch:

Bundesministerium
für Wirtschaft
und Energie

aufgrund eines Beschlusses
des Deutschen Bundestages

Data availability Non-digital data support this study.

Declarations

Competing interests The authors declare no competing interests.

References

1. Barsoum Z, Jonsson B (2011) Influence of weld quality on the fatigue strength in seam welds. Eng Fail Anal 18(3):971–979. https://doi.org/10.1016/j.engfailanal.2010.12.001
2. Haselibozchaloee D, Correia J, Mendes P, de Jesus A, Berto F (2022) A review of fatigue damage assessment in offshore wind turbine support structure. Int J Fatigue 164:107145. https://doi.org/10.1016/j.ijfatigue.2022.107145
3. Amirafshari P, Barltrop N, Wright M, Kolios A (2021) Weld defect frequency, size statistics and probabilistic models for ship structures. Int J Fatigue 145:106069. https://doi.org/10.1016/j.ijfatigue.2020.106069
4. Maiorana E, Aloisio A, Tasse V, Briseghella B (2024) Prediction of fatigue life of a bolted joint in railway steel arch bridge using multiaxial fatigue criteria. Eng Fail Anal 166:108908. https://doi.org/10.1016/j.engfailanal.2024.108908
5. Maddox SJ, Zhang Y-H (2008) Comparison of fatigue of girth-welds in full-scale pipes and small-scale strip specimens. In: Volume 5: Materials technology; CFD and VIV. ASMEDC; p. 75–85.
6. Madia M, Zerbst U, Th. Beier H, Schork B (2018) The IBESS model – elements, realisation and validation. Engineering Fracture Mechanics ;198:171–208.https://doi.org/10.1016/j.engfracmech.2017.08.033
7. Renken F, Bock und Polach RUF von, Schubnell J, Jung M, Oswald M, Rother K et al (2021) An algorithm for statistical evaluation of weld toe geometries using laser triangulation.

International Journal of Fatigue. 149:106293. https://doi.org/10.1016/j.ijfatigue.2021.106293
8. Braun M, Ahola A, Milaković A-S, Ehlers S (2022) Comparison of local fatigue assessment methods for high-quality butt-welded joints made of high-strength steel. Forces in Mechanics 6:100056. https://doi.org/10.1016/j.finmec.2021.100056
9. European Commit-2023-EN ISO 5817_2023 Welding.
10. Glienke R, Kalkowsky F, Hobbacher AF, Holch A, Thiele M, Marten F et al (2024) Evaluation of the fatigue resistance of butt-welded joints in towers of wind turbines — a comparison of experimental studies with small scale and component tests as well as numerical based approaches with local concepts. Weld World 68(5):1143–1168. https://doi.org/10.1007/s40194-023-01630-3
11. Hobbacher AF, Kassner M (2012) On relation between fatigue properties of welded joints, quality criteria and groups in ISO 5817. Weld World 56(1112):153–169
12. Schubnell J, Konidena SK, Jung M, Braun M, Ehlers S, Madia M et al (2024) Approach for the probabilistic fatigue assessment of welded joints based on the local geometry of the weld seam. Fatigue Fract Eng Mater Struct 47(1):88–107. https://doi.org/10.1111/ffe.14170
13. Shojai S, Schaumann P, Ghafoori E (2024) Micro-support effect consideration in fatigue analysis of corroded steel based on real surface geometry. J Constr Steel Res 212:108259. https://doi.org/10.1016/j.jcsr.2023.108259
14. Schork B, Kucharczyk P, Madia M, Zerbst U, Hensel J, Bernhard J et al (2018) The effect of the local and global weld geometry as well as material defects on crack initiation and fatigue strength. Eng Fract Mech 198:103–122. https://doi.org/10.1016/j.engfracmech.2017.07.001
15. Niraula A, Remes H, Lehto P (2023) Local weld geometry-based characterization of fatigue strength in laser-MAG hybrid welded joints. Weld World 67(6):1527–1544. https://doi.org/10.1007/s40194-023-01488-5
16. Schork B, Zerbst U, Kiyak Y, Kaffenberger M, Madia M, Oechsner M (2020) Effect of the parameters of weld toe geometry on the FAT class as obtained by means of fracture mechanics-based simulations. Weld World 64(6):925–936. https://doi.org/10.1007/s40194-020-00874-7
17. Braun M, Neuhäusler J, Denk M, Renken F, Kellner L, Schubnell J et al (2022) Statistical characterization of stress concentrations along butt joint weld seams using deep neural networks. Appl Sci 12(12):6089. https://doi.org/10.3390/app12126089
18. Braun M, Kellner L, Schreiber S, Ehlers S (2022) Prediction of fatigue failure in small-scale butt-welded joints with explainable machine learning. Procedia Struct Integr 38:182–191. https://doi.org/10.1016/j.prostr.2022.03.019
19. Braun M, Kellner L (2022) Comparison of machine learning and stress concentration factors-based fatigue failure prediction in small-scale butt-welded joints. Fatigue Fract Eng Mater Struct 45(11):3403–3417. https://doi.org/10.1111/ffe.13800
20. Shojai S, Schönamsgruber F, Köhler M, Ghafoori E (2025) Impact of accelerated corrosion on weld geometry, hardness and residual stresses of offshore steel joints over time. Mater Des 251:113578. https://doi.org/10.1016/j.matdes.2024.113578
21. Braun M (2022) Statistical analysis of sub-zero temperature effects on fatigue strength of welded joints. Weld World 66(1):159–172. https://doi.org/10.1007/s40194-021-01207-y
22. Braun M, Baumgartner J, Hofmann G, Drebenstedt K, Bauer NM, Bakhschi H (2023) A statistical assessment of the fatigue strength improvement of butt-welded joints by flush grinding. Weld World 67(10):2345–2359. https://doi.org/10.1007/s40194-023-01569-5
23. Schubnell J, Jung M, Le CH, Farajian M, Braun M, Ehlers S et al (2020) Influence of the optical measurement technique and evaluation approach on the determination of local weld geometry parameters for different weld types. Weld World 64(2):301–316. https://doi.org/10.1007/s40194-019-00830-0
24. Braun M, Schubnell J, Hultgren G (2025) Guideline for digital visual inspection (D-TV): part 1: determination of local geometrical parameters of welded joints. International Institute of Welding IIW-Doc. XIII-3153–2025
25. Hobbacher AF, Baumgartner J (2024) Recommendations for fatigue design of welded joints and components. Cham: Springer Nature Switzerland;
26. Shojai S, Brömer T, Ghafoori E, Schaumann P (2024) Application of local fatigue approaches on corroded welded joints with consideration of weld geometry and residual stresses. Theoret Appl Fract Mech 129:104215. https://doi.org/10.1016/j.tafmec.2023.104215
27. DVS verband (2019) Empfehlungen für die Durchführung, Auswertung und Dokumentation von Schwingfestigkeitsversuchen an Schweißverbindungen metallischer Werkstoffe: Merkblatt DVS 2403
28. Da Anderson TW D (1952) Asymptotic theory of certain goodness of fit criteria based on stochastic processes. 23.
29. Engamn S, Cousineau D (2011) Comparing distributions: the two-sample Anderson-Darling test as an alternative to the Kolmogorov-Smirnoff test. Journal of Applied Quantitative Methods. 3(3).
30. Kim D, Kim D-Y, Ko T, Hwan LS (2025) Physics-informed Gaussian process regression model for predicting the fatigue life of welded joints. Int J Fatigue 190:108644. https://doi.org/10.1016/j.ijfatigue.2024.108644
31. Tang K, Cui C, Li Y, Yuan X, Zhang Q, Yang Y (2025) Investigation of fatigue damage evolution mechanism in Q500qENH weathering steel welded joints with corroded surface morphology. Int J Fatigue 200:109116. https://doi.org/10.1016/j.ijfatigue.2025.109116
32. Ratner B (2009) The correlation coefficient: its values range between +1/−1, or do they? J Target Meas Anal Mark 17(2):139–142. https://doi.org/10.1057/jt.2009.5